Available online at www.sciencedirect.com

ScienceDirect

IFAC-PapersOnLine 48-28 (2015) 886–891

Experiment design for improved frequency domain subspace system identification of continuous-time systems

Majid Khorsand Vakilzadeh*, Vahid Yaghoubi*, Tomas McKelvey, Thomas Abrahamsson*, Lennart Ljung*****

**Department of applied mechanics, Chalmers University of Technology, SE-41296 Göteborg, Sweden (e-mail: yaghoubi@chalmers.se)*
***Department of signals and systems, Chalmers University of Technology, SE-41296 Göteborg, Sweden*
****Department of Electrical Engineering, Linköping University, S-58183, Linköping, Sweden*

Abstract: A widely used approach for identification of linear, time-invariant, MIMO (multi-input/multi output) systems from continuous-time frequency response data is to solve it in discrete-time domain using subspace based identification algorithm incorporated with a bilinear transformation. However, the bilinear transformation maps the distribution of the frequency lines from continuous-time domain to discrete-time domain in a non-linear fashion which may make identification algorithm to be ill-conditioned. In this paper we propose a solution to get around this problem by designing a dedicated frequency sampling strategy. Promising results are obtained when the algorithm is applied to synthetic data from a 6DOF mass-spring model.

Keywords: System identification, Subspace methods, Frequency responses, Frequency sampling strategy, Bias reduction.

1. INTRODUCTION

Recently, identification and control of large flexible structures have received considerable attention, Nayeri et al. (2008), Sirca Jr et al. (2012). This type of system is also frequently encountered in the modal analysis area of mechanical engineering, in which the dynamic properties of components or full systems are searched for by vibration testing. Typically such systems are lightly damped and quite often, as in the system analysis and control design of mechanical structures, high-order models with many inputs and outputs are needed.

The state-space model is one of the most well-known models that most modern multivariable control design techniques are based on. Methods which identify state-space models by means of geometrical properties of the input and output sequences are commonly known as subspace methods and have received much attention in the literature, see Viberg (1995) for a survey of time domain techniques. One of the advantages with subspace methods is that an estimate is calculated without any non-linear parametric optimization. In classical prediction error minimization, Ljung (1999), such a step is necessary for most model structures. The second advantage is that there is no difference between multi-input, multi-output (MIMO) system identification and SISO system identification for a subspace-based algorithm.

In this paper we consider the case when data is given in the frequency domain, i.e. the linear dynamical system is excited by a pure sinusoidal signal and the output has settled to a stationary sinusoidal signal, the complex value of the transfer function at the specific excitation frequency is determined by comparing the amplitudes and phases of the input and output signals, respectively. In a number of applications, particularly when modeling flexible structures, it is common to perform dynamic testing with frequency band-limited stimulus and fit models in the frequency domain, McKelvey et al. (1997), Schoukens et al. (1991). The frequency range of interest usually starts at a low frequency determined by the limitation of the vibration sensors and end at a frequency determined by the spectrum of the system loading under normal operating conditions. A few subspace based algorithms formulated in the frequency domain has appeared recently, McKelvey (2002), McKelvey et al. (1996), Overschee et al. (1996). In McKelvey et al. (1996), state-space subspace methods are discussed for discrete-time systems when data are uniformly or nonuniformly spaced in frequency. It was shown that the algorithm for uniformly spaced data is consistent but the algorithm for nonuniformly spaced data is strongly consistent if weighting strategy is employed requiring the noise covariance function to be known.

In this paper we are interested in applying the subspace based estimation methodology to estimate continuous-time state-space models from frequency domain data. We do this by employing the bilinear transformation methodology coupled with a subspace-based identification method, as described in McKelvey et al. (1996). In short, the method involves a pre-warping of the frequency scale of the data, the identification of a discrete-time state-space model and a bilinear transformation to arrive at the final continuous-time state-space model. Using other transformations, like the zero-order-hold transformation, is not suitable since the data is collected using sinusoidal excitation at a discrete set of frequencies.

Besides the issues with consistency when the data is non-uniformly spaced in frequency the subspace method is also, numerically, more sensitive. In this paper we discuss how the excitation frequencies should be selected in order to obtain a numerically well-conditioned estimation problem.

10.1016/j.ifacol.2015.12.242

In the rest of this section, after a brief review of the mathematical formulation for the bilinear transformation, we state how this transformation can result in biased estimations.

1.1 Mathematical preliminaries

Consider a stable, time-invariant, continuous-time and linear system of order n in state-space form

$$\begin{aligned}\frac{d}{dt}\mathbf{x}(t) &= \mathbf{A}^c\mathbf{x}(t) + \mathbf{B}^c\mathbf{u}(t)\\ \mathbf{y}(t) &= \mathbf{C}^c\mathbf{x}(t) + \mathbf{D}^c\mathbf{u}(t)\end{aligned} \tag{1}$$

where $\boldsymbol{y}(t) \in \Re^p$, $\boldsymbol{x}(t) \in \Re^n$ and $\boldsymbol{u}(t) \in \Re^m$. Whenever the input vector is exponentially bounded, the Laplace transform can be used to write the transfer function of model (1) as

$$\mathbf{G}^c(s) = \mathbf{C}^c(s\mathbf{I} - \mathbf{A}^c)^{-1}\mathbf{B}^c + \mathbf{D}^c \tag{2}$$

One way to transform the model (2) to the corresponding discrete-time model is to employ bilinear (also called Tustin) transformation. The bilinear transformation maps the complex values in the s domain to the z domain as

$$s = \frac{2(z-1)}{T(z+1)} \tag{3}$$

where T is a parameter in which the user is free to specify under the constraint that $2/T$ is not a pole of the continuous-time system. It also can be seen as a sort of sampling period. The important feature of the bilinear transformation is that the frequency response is invariant if we prewarp the frequency scale. Let the continuous-time transfer function be evaluated at $j\omega_k^c$ and let the bilinear transformed discrete-time transfer function be evaluated at $e^{j\omega_k}$, then it holds that

$$\mathbf{G}^c(j\omega_k^c) = \mathbf{G}^c\left(\frac{2(e^{j\omega_k}-1)}{T(e^{j\omega_k}+1)}\right) = \mathbf{G}(e^{j\omega_k}) \tag{4}$$

If $\tan(\omega_k/2) = \omega_k^c T/2$. Hence, given samples of a continuous-time transfer function $\boldsymbol{G}_k^c$ at frequencies ω_k^c, the samples of the corresponding bilinear transformed discrete-time transfer function $\mathbf{G}_k$ can be obtained simply as

$$\mathbf{G}_k = \mathbf{G}_k^c, \qquad k = 1,\ldots,M \tag{5}$$

$$\omega_k = 2\mathrm{atan}\left(\frac{\omega_k^c T}{2}\right), \qquad k = 1,\ldots,M \tag{6}$$

where atan denotes the inverse of tan. For state-space models, the transformed discrete-time model can be described, McKelvey et al. (1996), as

$$\begin{aligned}\mathbf{x}(k+1) &= \mathbf{A}\mathbf{x}(k) + \mathbf{B}\mathbf{u}(k)\\ \mathbf{y}(k) &= \mathbf{C}\mathbf{x}(k) + \mathbf{D}\mathbf{u}(k)\end{aligned} \tag{7}$$

where

$$\begin{aligned}&\mathbf{A} = \left(\frac{2}{T}\mathbf{I} + \mathbf{A}^c\right)\left(\frac{2}{T}\mathbf{I} - \mathbf{A}^c\right)^{-1},\ \mathbf{B} = \frac{2}{\sqrt{T}}\left(\frac{2}{T}\mathbf{I} - \mathbf{A}^c\right)^{-1}\mathbf{B}^c\\ &\mathbf{C} = \frac{2}{\sqrt{T}}\mathbf{C}^c\left(\frac{2}{T}\mathbf{I} - \mathbf{A}^c\right)^{-1},\ \mathbf{D} = \mathbf{D}^c + \mathbf{C}^c\left(\frac{2}{T}\mathbf{I} - \mathbf{A}^c\right)^{-1}\mathbf{B}^c\end{aligned} \tag{8}$$

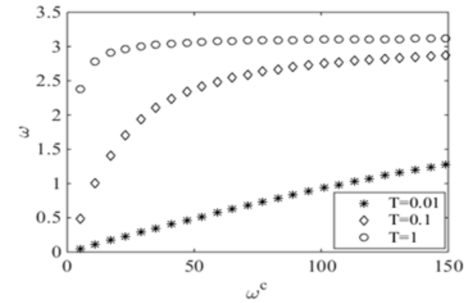

Fig. 1. Frequency mapping from continuous domain frequency scale to discrete domain for different T.

The inverse transformation can be applied to convert a discrete-time model to the corresponding continuous-time model.

1.2 Problem Statement

Given noise-corrupted samples of the continuous-time transfer function at M frequency points ω_k^c; identify a state space model (1) with transfer function $\hat{\mathbf{G}}_M^c$ such that with probability one

$$\lim_{M\to\infty}\left\|\hat{\mathbf{G}}_M^c - \mathbf{G}\right\|_\infty = \mathbf{0} \tag{9}$$

where $\|\mathbf{X}\|_\infty = \sup_{0\le\omega^c\le\infty}\sigma_1(\mathbf{X}(j\omega^c))$ and σ_1 denotes the largest singular value.

It is well known that the parameter estimation problem is better conditioned for discrete-time transfer functions since powers of $e^{j\omega_k}$ form a natural orthogonal basis, McKelvey et al. (1996). To this target, the bilinear transformation of (5) and (6) gives the samples of the transfer function in the discrete-time domain. This study employs the identification algorithms proposed in McKelvey et al. (1996) to derive a discrete-time model from samples of the frequency response in the discrete domain. Again using the bilinear transformation the discrete-time model can be transformed back to the continuous-time domain.

However, the frequency mapping (6) used in conjunction with the bilinear transformation prewarps the frequency scale in a non-linear way such that the frequency samples in the discrete-time domain are nonequidistantly spaced if the frequency samples in the continuous-time domain are equidistant. This suggests to employ the algorithm proposed by McKelvey et al. (1996) for arbitrary frequency spacing. To keep this algorithm consistent a weighting matrix has been derived based on *a priori* knowledge of the relative variance of the noise over the frequencies. Although the algorithm is consistent, in the finite data case it will result in a biased estimate and it turns out that the size of this bias is dependent on the numerical conditioning of the problem. The frequency mapping (6) often leads to have a majority of frequency lines concentrated in a specific region of the frequency scale in the discrete domain, see Fig. 1. This figure illustrates the mapping of the frequency range 20 to 150 rad/s with steps of 6 rad/s to the corresponding frequencies for the discrete-time model using (6) with different T. This peculiarity of the frequency mapping (6) may lead to an ill-conditioned weighting matrix and make the bias in finite data case to increase. To alleviate this problem, the present study introduces a dedicated frequency sampling strategy to improve the consistency of the frequency domain subspace identification algorithm for continuous-time systems.

2. IDENTIFICATION METHOD

This section begins with the description of the frequency domain identification algorithm in the discrete-time domain. Afterwards, two different methods are investigated to improve performance of the identification algorithm in the presence of noise. The first method, Gunnarsson et al. (2007) and McKelvey et al. (1996), which is a pre-whitening technique attempts to make the identification algorithm consistent for arbitrarily distanced frequency lines in the discrete-time domain. The second method proposes a dedicated frequency sampling strategy which samples the continuous-time transfer function at the frequencies corresponding to equidistantly spaced frequencies in the discrete-time domain.

2.1 Subspace identification in discrete-time domain

We assume we have a set of measured frequency function matrices $\mathbf{G}(j\omega_k), k=1,...,M$. By introducing the notation

$$\mathbf{X}(\omega)=\left(e^{j\omega}-\mathbf{A}\right)^{-1}\mathbf{B} \tag{10}$$

we can describe the measurements in state-space form as

$$\begin{aligned} e^{j\omega}\mathbf{X}(\omega) &= \mathbf{A}\mathbf{X}(\omega)+\mathbf{B} \\ \mathbf{G}\left(e^{j\omega}\right) &= \mathbf{C}\mathbf{X}(\omega)+\mathbf{D}+\mathbf{N}_\omega \end{aligned} \tag{11}$$

where $\mathbf{N}_\omega$ is a matrix with the measurement errors with elements that are zero mean independent random variables with identical complex Gaussian distribution. Now, let us introduce the vector

$$\mathbf{W}(\omega)=\left[1\; e^{j\omega}\; e^{j2\omega}\;\ldots\; e^{j\omega(q-1)}\right]^{\mathrm{T}} \tag{12}$$

and the lower triangular block-Toeplitz matrix

$$\mathbf{\Gamma}_q=\begin{bmatrix} \mathbf{D} & \mathbf{0} & \cdots & \mathbf{0} \\ \mathbf{CB} & \mathbf{D} & \cdots & \mathbf{0} \\ \vdots & \vdots & \ddots & \vdots \\ \mathbf{CA}^{q-2}\mathbf{B} & \mathbf{CA}^{q-3}\mathbf{B} & \cdots & \mathbf{D} \end{bmatrix} \in \Re^{qp\times mq} \tag{13}$$

By recursive use of (11) we obtain

$$\mathbf{W}(\omega)\otimes\mathbf{G}\left(e^{j\omega}\right)=\mathbf{O}_q\mathbf{X}(\omega)+\mathbf{\Gamma}_q(\mathbf{W}(\omega)\otimes\mathbf{I}_m)+\mathbf{W}(\omega)\otimes\mathbf{N}_\omega \tag{14}$$

where $\otimes$ denotes the standard Kronecker product, Kailath (1980) and $\mathbf{O}_q=[\mathbf{C}\quad \mathbf{CA}\quad \cdots\quad \mathbf{CA}^q]$. If M samples of the transforms are known we can collect all data into one complex matrix equation. Define the diagonalization operator for a sequence of matrices $\mathbf{z}_i$ of size $p\times m$ as

$$\operatorname{diag}(\mathbf{z}_1,\mathbf{z}_2,...,\mathbf{z}_M)=\begin{bmatrix} \mathbf{z}_1 & 0 & & 0 \\ 0 & \mathbf{z}_2 & \ddots & 0 \\ & \ddots & \ddots & \\ 0 & & 0 & \mathbf{z}_M \end{bmatrix} \tag{15}$$

which is a tall (or square) matrix of size $Mp\times Mm$. By introducing the additional matrices

$$\begin{aligned} \mathbf{W} &= \left[\mathbf{W}(\omega_1),\mathbf{W}(\omega_2),\cdots,\mathbf{W}(\omega_M)\right]\otimes\mathbf{I}_m \\ \mathbf{W}_p &= \left[\mathbf{W}(\omega_1),\mathbf{W}(\omega_2),\cdots,\mathbf{W}(\omega_M)\right]\otimes\mathbf{I}_p \\ \mathbf{G} &= \frac{1}{\sqrt{M}}\mathbf{W}_p\operatorname{diag}\left[\mathbf{G}\left(e^{j\omega_1}\right),\mathbf{G}\left(e^{j\omega_2}\right),\cdots,\mathbf{G}\left(e^{j\omega_M}\right)\right]\in\Re^{qp\times mM}, \\ \mathbf{N} &= \frac{1}{\sqrt{M}}\mathbf{W}_p\operatorname{diag}\left[n_1,n_2,\cdots,n_M\right]\in\Re^{qp\times mM}, \\ \mathbf{X} &= \frac{1}{\sqrt{M}}\left[\mathbf{X}(\omega_1),\mathbf{X}(\omega_2),\cdots,\mathbf{X}(\omega_M)\right]\in\Re^{n\times mM} \end{aligned} \tag{16}$$

and using (14) we arrive at the matrix equation

$$\mathbf{G}=\mathbf{O}_q\mathbf{X}+\mathbf{\Gamma}_p\mathbf{W}+\mathbf{N} \tag{17}$$

The identification scheme we employ to find a state-space model ($\hat{\mathbf{A}},\hat{\mathbf{B}},\hat{\mathbf{C}},\hat{\mathbf{D}}$) is based on a two-step procedure. First the relation (17) is used to consistently determine a matrix $\hat{\mathbf{O}}_q$, with a range space equal to the extended observability matrix $\mathbf{O}_q$. The second step is to remove the influence of the $\mathbf{\Gamma}_p\mathbf{W}$ term, which can be accomplished using a projection matrix $\mathbf{\Pi}^\perp$ projecting onto the nullspace of $\mathbf{W}$.

$$\mathbf{\Pi}^\perp=\mathbf{I}-\mathbf{W}^{\mathbf{H}}(\mathbf{W}\mathbf{W}^{\mathbf{H}})^{-1}\mathbf{W} \tag{18}$$

postmultiplying $\mathbf{G}$ with $\mathbf{\Pi}^\perp$ results in

$$\mathbf{G}\mathbf{\Pi}^\perp=\mathbf{O}_q\mathbf{X}\mathbf{\Pi}^\perp+\mathbf{N}\mathbf{\Pi}^\perp \tag{19}$$

Finally, we estimate a basis of the range space of $\mathbf{O}_q$ using the Singular Value Decomposition (SVD) of $\mathbf{G}\mathbf{\Pi}^\perp$ and partitioning it as

$$\mathbf{G}\mathbf{\Pi}^\perp=\begin{bmatrix}\hat{\mathbf{U}}_s & \hat{\mathbf{U}}_n\end{bmatrix}\begin{bmatrix}\hat{\mathbf{\Sigma}}_s & 0 \\ 0 & \hat{\mathbf{\Sigma}}_n\end{bmatrix}\begin{bmatrix}\hat{\mathbf{V}}_s^H \\ \hat{\mathbf{V}}_n^H\end{bmatrix} \tag{20}$$

where $\hat{\mathbf{U}}_\mathbf{s}$ contains the *n* principal left singular vectors and $\hat{\mathbf{\Sigma}}_\mathbf{s}$ the corresponding singular values. In the noise free case $\hat{\mathbf{\Sigma}}_n=0$ and there will exist a nonsingular matrix $\mathbf{T}_s$ such that

$$\mathbf{O}_q=\hat{\mathbf{U}}_s\mathbf{T}_s \tag{21}$$

By viewing $\hat{\mathbf{U}}_\mathbf{s}$ as an estimated observability matrix $\hat{\mathbf{O}}_q$ for some realizations the shift-invariance techniques described in Viberg (1995) can be used to compute the estimated $\hat{\mathbf{A}}$ and $\hat{\mathbf{C}}$. Finally $\hat{\mathbf{B}}$ and $\hat{\mathbf{D}}$ are determined by minimizing the 2-norm of the error

$$\hat{\mathbf{B}},\hat{\mathbf{D}}=\arg\min_{\mathbf{B},\mathbf{D}}V_M(\mathbf{B},\mathbf{D}) \tag{22}$$

where

$$V_M(\mathbf{B},\mathbf{D})=\sum_{k=1}^{M}\left\|\mathbf{G}-\hat{\mathbf{G}}(\omega_k,\mathbf{B},\mathbf{D})\right\|^2 \tag{23}$$

with

$$\hat{\mathbf{G}}(\omega_k,\mathbf{B},\mathbf{D})=\mathbf{D}-\hat{\mathbf{C}}(e^{j\omega_k}\mathbf{I}-\hat{\mathbf{A}})^{-1}\mathbf{B} \tag{24}$$

which has an analytical solution since the output $\hat{\mathbf{G}}$ is a linear function of both $\mathbf{B}$ and $\mathbf{D}$ assuming $\hat{\mathbf{A}}$ and $\hat{\mathbf{C}}$ are fixed. Hence once $\hat{\mathbf{A}}$ and $\hat{\mathbf{C}}$ are derived $\hat{\mathbf{B}}$ and $\hat{\mathbf{D}}$ is determined by linear regression.

2.2 Noise perturbation

In the presence of noise, $\hat{\mathbf{U}}_s$ forms a strongly consistent estimate of the range space of $\mathbf{O}_q$ if two conditions hold (w.p.1)

$$\text{I)}\ \lim_{M\to\infty} \underbrace{\mathbf{O}_q\mathbf{X}\mathbf{\Pi}^{\perp}(\mathbf{N}\mathbf{\Pi}^{\perp})^{\mathrm{H}}}_{\mathbf{S}(M)} = \mathbf{0} \tag{25}$$

$$\text{II)}\ \lim_{M\to\infty} \underbrace{\mathbf{N}\mathbf{\Pi}^{\perp}(\mathbf{N}\mathbf{\Pi}^{\perp})^{\mathrm{H}}}_{\mathbf{P}(M)} = \alpha\mathbf{I} \tag{26}$$

Based on the zero mean assumption and the boundedness of the moments of n_k, one can show that

$$\lim_{M\to\infty} [\mathbf{S}(M)]_{ij} = 0, \quad \text{w.p. 1} \quad \forall i, j. \tag{27}$$

Using the fact that $\mathbf{\Pi}^{\perp}(\mathbf{\Pi}^{\perp})^{\mathrm{H}} = \mathbf{\Pi}^{\perp}$, $\mathbf{P}(M)$ in (26) can be rewritten as

$$\mathbf{P}(M) = \mathbf{N}\mathbf{\Pi}^{\perp}\mathbf{N}^{\mathrm{H}} \tag{28}$$

McKelvey et al. (1996) showed that $\mathbf{P}(M)$ converges to its expected value if M tends to infinity. Gunnarsson et al. (2007) derived an exact formulation for expectation of $\mathbf{P}(M)$ in (28) as

$$\mathrm{E}\left\{\mathbf{N}\mathbf{\Pi}^{\perp}\mathbf{N}^{\mathrm{H}}\right\} = \sigma_n^2(\mathbf{W}\mathbf{\Lambda}_{\mathbf{\Pi}^{\perp}}\mathbf{W}^{\mathrm{H}})\otimes\mathbf{I}_m \tag{29}$$

Here, $\mathbf{\Lambda}_{\mathbf{\Pi}^{\perp}}$ is a diagonal matrix whose diagonal elements are identical to those in $\mathbf{\Pi}^{\perp}$. Sufficient condition to guarantee that $(\mathbf{W}\mathbf{\Lambda}_{\mathbf{\Pi}^{\perp}}\mathbf{W}^{\mathrm{H}})\otimes\mathbf{I}_m$ is proportional to identity is to sample data equidistantly in frequency covering the full unit circle $\omega_k = 2\pi k / M, k = 0,\ldots,M-1$.

However, this condition does not often hold for identification of the continuous-time systems. The reason for this is twofold. First, the sampling frequencies in the continuous-time domain will be mapped to arbitrarily spaced frequency samples in discrete-time domain due to prewarping of the frequency scale in (6). Second, the continuous-time transfer function is usually measured in limited frequency range which does not fully cover the entire unit circle in the discrete domain. Consequently, the $\mathbf{P}(M)$ in (26) is not proportional to identity and will hence perturb the basis of the range space of the observability matrix. To alleviate this problem, we investigate a pre-whitening technique in the next section.

2.2.1 Noise diagonalization matrix

This section investigates the pre-whitening technique presented by McKelvey et al. (1996) and Gunnarsson et al. (2007) to make the noise matrix in (29) proportional to the identity matrix using a weighting matrix $\mathbf{K}^{-1}$ satisfying

$$\mathbf{I} = \mathbf{K}^{-1}(\mathbf{W}\mathbf{\Lambda}_{\mathbf{\Pi}^{\perp}}\mathbf{W}^{\mathrm{H}})\otimes\mathbf{I}_m\mathbf{K}^{-\mathrm{H}} \tag{30}$$

or identically

$$\mathbf{K}\mathbf{K}^{\mathrm{H}} = (\mathbf{W}\mathbf{\Lambda}_{\mathbf{\Pi}^{\perp}}\mathbf{W}^{\mathrm{H}})\otimes\mathbf{I}_m \tag{31}$$

To obtain $\mathbf{K}$, the SVD is used to compute the factorization

$$(\mathbf{W}\mathbf{\Lambda}_{\mathbf{\Pi}^{\perp}}\mathbf{W}^{\mathrm{H}})\otimes\mathbf{I}_m = \mathbf{U}_{\mathrm{W}}\mathbf{\Sigma}_{\mathrm{W}}\mathbf{U}_{\mathrm{W}}^{\mathrm{H}} \tag{32}$$

which results in

$$\mathbf{K}^{-1} = \mathbf{\Sigma}_{\mathrm{W}}^{-1/2}\mathbf{U}_{\mathrm{W}}^{\mathrm{H}},\ \ \mathbf{K} = \mathbf{U}_{\mathrm{W}}\mathbf{\Sigma}_{\mathrm{W}}^{1/2} \tag{33}$$

Finally, the SVD of $\mathbf{K}^{-1}\mathbf{G}\mathbf{\Pi}^{\perp}$ is partitioned into a signal and noise subspace

$$\mathbf{K}^{-1}\mathbf{G}\mathbf{\Pi}^{\perp} = \begin{bmatrix}\hat{\mathbf{U}}'_s & \hat{\mathbf{U}}'_n\end{bmatrix}\begin{bmatrix}\hat{\mathbf{\Sigma}}'_s & 0 \\ 0 & \hat{\mathbf{\Sigma}}'_n\end{bmatrix}\begin{bmatrix}\hat{\mathbf{V}}'^{\mathrm{H}}_s \\ \hat{\mathbf{V}}'^{\mathrm{H}}_n\end{bmatrix} \tag{34}$$

and $\mathbf{K}\hat{\mathbf{U}}'_s$ is taken as an estimate of $\mathbf{O}_q$.

2.2.2 Frequency Sampling Strategy

In many scenarios, especially when the number of samples in the frequency domain is high or the estimation is based on a narrow frequency interval, the matrix $(\mathbf{W}\mathbf{\Lambda}_{\mathbf{\Pi}^{\perp}}\mathbf{W}^{\mathrm{H}})\otimes\mathbf{I}_m$ becomes ill-conditioned, Gunnarsson et al. (2007). To circumvent this problem, we propose a dedicated frequency sampling strategy where the frequency components, $\omega_1^c,\ldots,\omega_M^c$, for the continuous-time model are selected such that they are mapped into an equidistant frequency grid for the discrete-time model. Moreover, by selecting a proper T in the frequency mapping, it is even possible to use the maximum feasible range between $[0,\pi]$ for the discrete-time model. This results in an improvement of the condition number of the matrix $(\mathbf{W}\mathbf{\Lambda}_{\mathbf{\Pi}^{\perp}}\mathbf{W}^{\mathrm{H}})\otimes\mathbf{I}_m$. The following algorithm explains the proposed frequency sampling technique.

1) Given the frequency range of interest in the continuous-time domain, $[\omega_1^c,\omega_M^c]$ and the desired number of frequency lines.
2) Determine T in (6) such that
$$T_o = \arg\max_{\mathrm{T}}\left|2\,\mathrm{atan}(\frac{\omega_1^c T}{2}) - 2\,\mathrm{atan}(\frac{\omega_M^c T}{2})\right| \tag{35}$$
3) Calculate the corresponding lower and upper bound of the frequency range for the discrete-time model using T_o;
$$\omega_1 = 2\,\mathrm{atan}(\frac{\omega_1^c T_o}{2}),\ \ \omega_M = 2\,\mathrm{atan}(\frac{\omega_M^c T_o}{2}) \tag{36}$$
4) Design equidistant frequencies at the DFT grid covering the full unit circle $\Omega_k = 2\pi k / M_F, k = 0,\ldots,M_F - 1$ where
$$M_F = \left[\frac{2\pi M}{\omega_M - \omega_1}\right] \tag{37}$$
Here, $[x]$ rounds x towards the nearest integer number.
5) Select the set of M first frequencies, $\Omega_l,\Omega_{l+1},\ldots,\Omega_{l+M}$, larger than ω_1.

6) Map $\Omega_l, \Omega_{l+1}, ..., \Omega_{l+M}$ back to the continuous-time domain using

$$\omega_k^c = \frac{2}{T}\tan(\frac{\Omega_{l+k}}{2}),\ k = 1, ..., M \quad (38)$$

This algorithm will then be used in the experiment design stage in order to measure the samples of the continuous-time transfer functions $\hat{\mathbf{G}}_k^c$ at frequencies ω_k^c.

3. RESULTS AND DISCUSSIONS

This section deals with identification of linear models from synthetic data, presented in Khorsand Vakilzadeh et al. (2014). The data stemmed from a 6DOF mass-spring system illustrated in Fig. 2. The parameter of the system is listed in Table 1, a relative modal damping of 1% is assigned to all modes of the model. The reference continuous-time transfer functions $\mathbf{G}^{\text{ref}}$ is obtained by exciting the system through the sixth degree of freedom and the acceleration data, simulated in this study, is measured at all degrees of freedom within the frequency range [3, 23] Hz with 2000 frequency lines. The synthetic data is the acceleration data contaminated with a small amount of white noise, up to 1.8% RMS noise-to-signal ratio. Fig. 3 depicts the amplitude of the measured FRF data with 1% RMS noise-to-signal ratio (NSR).

The synthetic data has been identified using three algorithms. (I) Ordinary algorithm: the subspace method without weighting in the SVD using (20) and with equidistant frequencies in the continuous-time domain; (II) weighting algorithm: the subspace method with weighting in the SVD using (34) and equidistant frequencies in the continuous-time domain; (III) selected frequency algorithm: the subspace method without weighting in the SVD and with the designed sampling frequencies in (38) corresponding to equidistant frequencies in the discrete-time domain at the DFT grid. To assess the performance of the three algorithms we perform a Monte-Carlo simulation where we repeat the experiment n_{MC}=100 times and estimate a new model for each dataset. The misfit between the reference and estimated transfer function

$$\left\|\mathbf{G}^{\text{ref}} - \hat{\mathbf{G}}\right\|_\infty = \max_{\omega_k}(\left|\mathbf{G}_k^{\text{ref}} - \hat{\mathbf{G}}(j\omega_k)\right|),\ k = 1, ..., M \quad (39)$$

and the root-mean-squared error (RMSE) of the estimated system's pole

$$\text{RMSE} = \sqrt{\frac{1}{n_{\text{MC}}}\sum_{i=1}^{n_{\text{MC}}}(\text{P}^{\text{ref}} - \hat{P}_i)\overline{(\text{P}^{\text{ref}} - \hat{P}_i)}} \quad (40)$$

in which P^{ref} is one of the poles of reference model and $\hat{P}_i$ is the poles of the ith estimated model, are used as two quality measures. Fig. 4 presents the scatterplot of estimated poles obtained by the use of ordinary subspace identification algorithm of the synthetic FRF with 1% RMS NSR.

It indicates bias in the system's pole location. Since the 4th pole show the most bias in the estimation, we will study only the variation in its estimations.

Bias, variance and RMSE of the 4th pole of the estimated systems are presented in Fig. 5 (A, B and C) respectively. Results indicate bias introduced by the ordinary subspace identification algorithm.

By increasing NSR the bias increased at a high rate. Therefore, the ordinary subspace identification was employed only to treat synthetic data with NSR less than 1%. Using either of weighting or selected frequency subspace identification algorithms can reduce the bias.

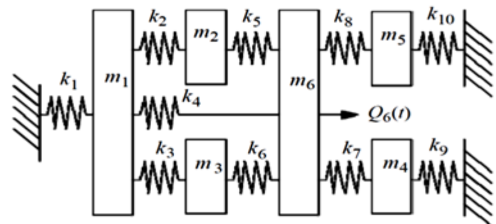

Fig. 2. 6DOF mass-spring system with 16 parameters

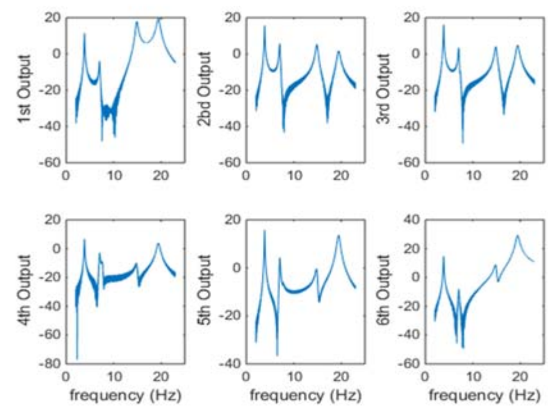

Frequency (Hz)

Fig. 3. Magnitude of the simulated FRFs (acceleration as output) for 1% RMS noise-to-signal ratio.

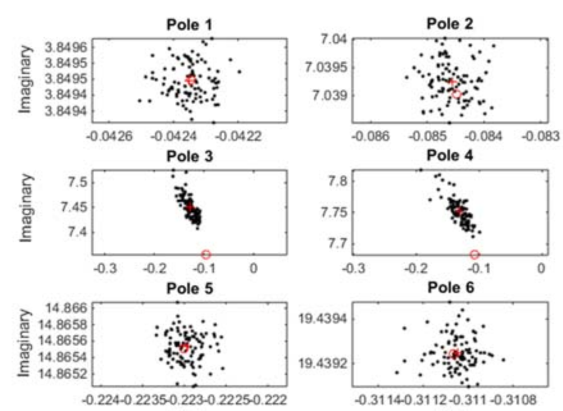

Fig. 4. Scatterplot of the estimated poles using subspace based identification method with equidistant frequency grid in continuous-time model. Red "o" is the reference pole, red "+" is the mean value of the estimated poles and black dot is the spread of the estimated pole.

Table 1: parameter values; stiffnesses (k_i) in kN/m and masses (m_i) in kg.

k_1	k_2	k_3	k_4	k_5	k_6	k_7	k_8	k_9	k_{10}	m_1	m_2	m_3	m_4	m_5	m_6
3600	1725	1200	2200	1320	1330	1500	5250	3600	850	1	1.4	1.2	2.2	2.5	0.9

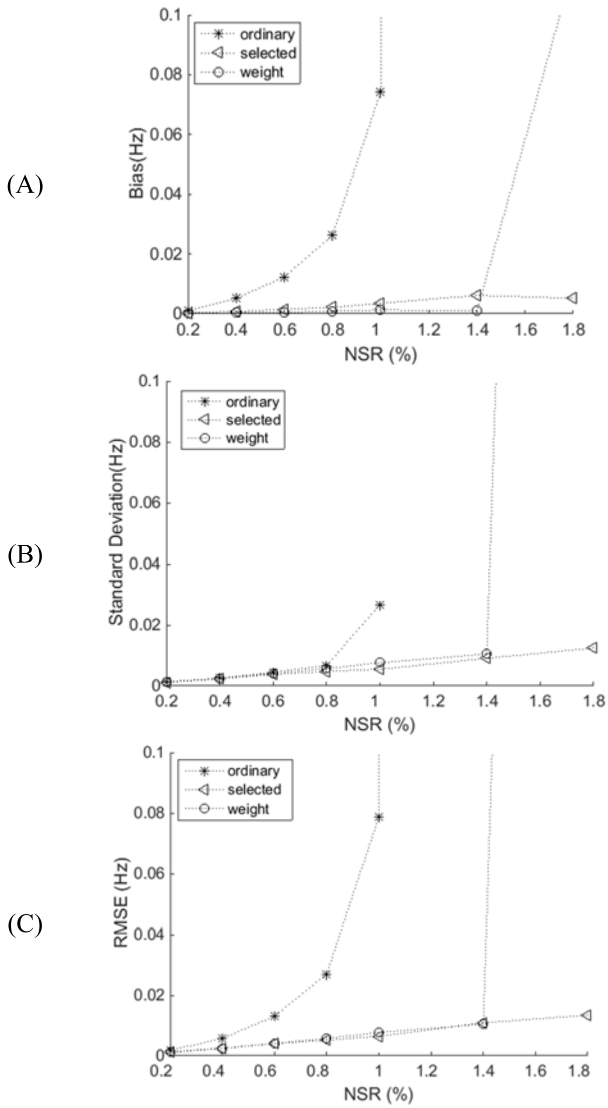

Fig. 5. Bias (A), standard deviation (B) and RMSE (C) of the estimated 4th pole

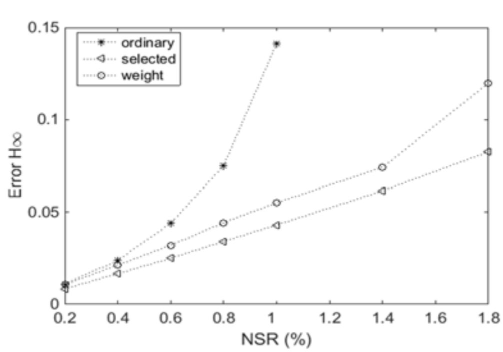

Fig. 6. Misfit between the reference and estimated transfer functions in H_∞ sense

The weighting algorithm resulted in poor pole estimation in presence of noise with RMS NSR more than 1.4%. Fig. 5C shows that selected frequency algorithm is more consistent in the presence of noise. Fig. 6, showing misfit between estimated transfer functions and the reference in H_∞ sense, indicates that selected frequency subspace identification algorithm gives more accurate results.

4. CONCLUSIONS

In this paper, we have developed a new frequency sampling strategy to measure transfer function for continuous-time subspace based system identification. This method allows to improving the accuracy of the identification algorithm by a proper experiment design. From experimental studies, the algorithm shows a promising performance comparing to a bias-compensation scheme which derives a weighting matrix from *a priori* knowledge of relative variance of the noise over the frequencies.

ACKNOWLEDGMENTS

Supported by the ERC advanced grant LEARN, no 287381, funded by the European Research Council.

REFERENCES

Gunnarsson, J. and McKelvey, T. (2007). Reducing noise sensitivity in F-ESPRIT using weighting matrices. *Proceedings of 15th European signal processing conference*, Poznan, Poland.

Kailath, T. (1980). *Linear systems*. Englewood Cliffs, New Jersey, Prentice Hall.

Khorsand Vakilzadeh, M., Yaghoubi, V., Johansson, A. and Abrahamsson, T. (2014). Manifold Metropolis adjusted Langevin algorithm for high-dimensional Bayesian FE. *Proceedings of the 9th international conference on structural dynamics, EURODYN*, Porto, Portogual.

Ljung, L. (1999). *System Identification: Theory for the User*. Englewood Cliffs, New Jersey, Prentice Hall.

McKelvey, T. (2002). Frequency domain identification methods. *Circuits Systems Signal Processing*, 21(1), 39-55.

McKelvey, T., Akçay, H. and Ljung, L. (1996). Subspace-based multivariable system identification from frequency response data. *IEEE tr. on Automatic Control*, 41(7), 960-979.

McKelvey, T., Akçay, H. and Ljung, L. (1996). Subspace-based multivariable system identification from frequency response data. *Automatic Control*, 41(7), 960-979.

McKelvey, T., Akçay, H. and Ljung, L. (1996). Subspace-based multivariable system identification from frequency response data. *IEEE Transactions on Automatic Control*, 41(7), 960-979.

McKelvey, T. and Ljung, L. (1997). Frequency domain maximum likelihood identification. *Proceedings of the 11th IFAC symposium on system identification*, Fukuoka, Japan.

Nayeri, R. D., Masri, S. F., Ghanem, R. G. and Nigbor, R. L. (2008). A novel approach for the structural identification and monitoring of a full-scale 17-story building based on ambient vibration measurements. *Smart Materials and Structures*, 17(2), 25006.

Overschee, V. P. and Moor, D. B. (1996). Continuous-time frequency domain subspace system identification. *Signal Processing*, 52(2), 179-194.

Schoukens, J. and Pintelon, R. (1991). *Identification of linear systems: a practical guideline to accurate modeling*. London, UK, Pergamon Press.

Sirca Jr, G. F. and Adeli, H. (2012). System identification in structural engineering. *Scientia Iranica*, 19(6), 1355-1364.

Viberg, M. (1995). Subspace-based methods for the identification of linear time-invariant systems. *Automatica*, 31(12), 1835-1851.